Pol. J. Environ. Stud. Vol. 30, No. 2 (2021), 1621-1629
DOI: *10.15244/pjoes/125769* ONLINE PUBLICATION DATE: 2020-12-02

Original Research

Hydroxyapatite-PEG/Fe_3O_4 Composite for Adsorption of Phenol from Aqueous Solution

Poedji Loekitowati Hariani*, Muhammad Said, Addy Rachmat, Sarah Permata Sari

Department of Chemistry, Faculty of Mathematics and Natural Sciences, Universitas Sriwijaya

Received: 12 May 2020
Accepted: 27 July 2020

Abstract

Hydroxyapatite-PEG/Fe_3O_4 composites were prepared using the co-precipitation method and applied for phenol removal from the solution. The composites synthesized within ratios of hydroxyapatite to Fe_3O_4 of 3:1, 2:1, and 1:1 at a fixed amount of polyethylene glycol. The properties of resulting materials were evaluated using XRD, FTIR, SEM-EDS, and VSM while the surface areas were calculated using the BET method. The effectiveness of the composites on phenol removal was studied, including contact time, solution pH, and initial concentration. Hydroxyapatite surface area decreased by the addition of Fe_3O_4 on the composites with ratios of 3:1, 2:1 and 1:1 from its initial value of 264.6 to 245.2, 237.3 and 201.4 $m^2 g^{-1}$, respectively. As the amount of the Fe_3O_4 impregnated increased, the magnetic properties increased to 44.1, 57.8, and 65.5 emu g^{-1}. A composite having a ratio of 2:1 was chosen for phenol adsorption due to its optimum combined properties, namely the surface area and magnetism. The Langmuir isotherm model best described the phenol adsorption by hydroxyapatite and the chosen composite resulting in adsorption capacities of 88.49 and 95.24 mg g^{-1}, respectively. The composite was found to be more effective, can be separated and easily regain using a permanent magnet. The pseudo-second order kinetics shows a higher correlation on describing the mechanism of phenol adsorption by both materials. The negative value of $\Delta G^0$and ΔH^0 shows that the adsorption process is spontaneous and exothermic.

Keywords: hydroxyapatite-PEG/Fe_3O_4, magnetic properties, adsorption, phenol

Introduction

Phenol is produced naturally from protein, humus, and lignin decomposed by bacteria [1]. Petrochemical, plastic, rubber, pesticide, pharmaceutical, resin, steel, and dye industries generally use it as raw material [2, 3]. Having high toxicity, hardness in biodegradability and mutagenic effect at high concentration makes it can cause serious impacts when discharged into the environment. Its presence in water can make the water's taste and odour to be unpleasant [1, 4]. Also, it can threaten aquatic organisms as it reaches a concentration of 1 mg L^{-1} [5]. So, its removal is urgent and necessary before discharged into the environment.

*e-mail:puji_lukitowati@mipa.unsri.ac.id

Several techniques have been developed to reduce phenol concentration in wastewater, among which are wet air oxidation [5], electrocoagulation [6], biological treatment [7], and adsorption methods [1,2,8]. The latter is conventional for wastewater treatment and removing phenol from solution for its effectiveness, low cost, and ease of implementation. *Luffa cylindrica* fibres [1], hydroxyapatite [2], carbon nanotubes [3] and carbon nanomaterials [4] are adsorbents used in this method. Hydroxyapatite (HA), a calcium phosphate-based material with a chemical formula of $Ca_{10}(PO_4)_6(OH)_2$ is generally used for tooth and bone implant. It can be used as an adsorbent due to its large surface area, good mechanical properties, low water solubility, stable oxidation and reduction processes, and cheapness [9]. It has been reported as an excellent adsorbent to organic and inorganic compounds such as phenol [2], dichromate [10], Pb [11], and Ni [12].

Recently, magnetic adsorbents draw attention for their usage for adsorbing and separating pollutants from wastewater. Modification of various adsorbents has been conducted to obtain magnetic ones including fly ash-$CoFe_2O_4$ to adsorb Malachite green dye [13], activated carbon- $CuFe_2O_4$ to adsorb Orange acid (II) dye [14], activated carbon-$CuFe_3O_4$ to remove Procion red dye [15], and $NiFe_2O_4/SiO_2$ to adsorb Ce(IV) [16]. Magnetic properties created on the adsorbents can increase the separation efficiency using a permanent magnet, the process of separating the adsorbent from the solution takes place quickly, and no filtration is necessary after wastewater treatment [17]. Fe_3O_4 is a ferrite material with a superparamagnetic property that is frequently used as an effective adsorbent. Feng et al. [18] reported that it could removal Pb, Zn, and Cu ions from the solution. Coated by humic acid, it is also reported having the capability of adsorbing phenol [19].

In this paper, we synthesized hydroxyapatite-PEG/Fe_3O_4 composites through the co-precipitation method. The addition of polyethylene glycol (PEG) aimed to control particle size and prevent agglomeration [20]. The composites were applied to the adsorption of phenol from the solution. The effect of contact time, solution pH, and initial concentration were studied. The adsorption isotherm and kinetics models of phenol also were evaluated.

Materials and Methods

Materials

Chemicals used in this research were phenol, $Ca(NO_3)_2$, $FeCl_3.6H_2O$, $FeCl_2.4H_2O$, NaOH, HCl, $(NH_4)_2HPO_4$, 4-aminoantipyrine, and Polyethylene glycol (PEG) (with a molar mass of 3500-4000 g mol^{-1}). Only phenol was purchased from Sigma-Aldrich, while the others were obtained from Merck-Millipore.

Synthesis of Hydroxyapatite

Hydroxyapatite was synthesised through the co-precipitation method. A precursor containing $Ca(NO_3)_2$ (0.5 M) as much as 500 mL was stirred and flowed by nitrogen at room temperature and then $(NH_4)_2HPO_4$ (0.387 M) was poured into the solution dropwise while the solution pH was kept at 11 using $(NH_4)OH$ solution. The mixture was stirred for an hour, and then the precipitate was collected through filtration.

Synthesis of Hydroxyapatite-PEG/Fe_3O_4 Composites

Hydroxyapatite-PEG/Fe_3O_4 composites were prepared through the co-precipitation method with ratios of hydroxyapatite to Fe_3O_4 of 3:1, 2:1 and 1:1. PEG was set in a fixed amount. The composite with a ratio of 1:1 was prepared by mixing PEG (5 g), hydroxyapatite (5 g), and distilled water (50 mL) flowed with nitrogen gas, all of which was stirred and heated at 70 °C on a hot-plate. Into this solution, a mixture of $FeCl_3.6H_2O$ (11.662 g) and $FeCl_2.4H_2O$ (4.292 g) in distilled water (50 mL) were added and homogenised. NaOH (1 M) was poured gradually to create a pH of 10 and form a dark precipitate. The precipitate was then separated by using a permanent magnet and washed using distilled water and ethanol for several times. The solid was dried up in an oven at 60 °C for 3 hours. Similar procedures were conducted for preparing composites with ratios of hydroxyapatite to Fe_3O_4 of 2:1 and 3:1. The reaction of the formation of Hydroxyapatite (HAp), PEG and Fe_3O_4 as follows:

$$2FeCl_3.6H_2O + FeCl_2.4H_2O + 8NaOH + HAp + PEG \rightarrow HAp\text{-}PEG/Fe_3O_4 + 8NaCl + 20H_2O$$

Hydroxyapatite and the composites characterization were conducted by Fourier transform infrared spectrophotometer (Thermo-Fisher Scientific Inc.) to evaluate their functional groups. The sample was mixed with KBr and made in pellets. The wavenumbers used were ranging from 400 to 3900 cm^{-1} to obtain transmittance percentage. An X-ray diffractometer (Rigaku Miniflex 600) was used in the analysis of phase using Cu Kα radiation as an X-ray source at λ 1.54056 Å and a range of 2*q* of 10-80°. Surface morphology was evaluated using a scanning electron microscope equipped with energy-dispersive X-ray spectroscopy (Shimadzu AA-700). The magnetic properties were determined using a vibrating sample magnetometer (Lakeshore 74004), while the surface area was calculated based on the BET method using data obtained from a surface area analyzer (ASAP 2020). The concentration of phenol was determined using 4-aminoanthypirine, which was detected using a UV-visible spectrophotometer (Biobase BK-UV1800 1600 UV-Vis) at a wavelength of 269 nm.

Adsorption Studies

The study of phenol adsorption was carried out using a composite with a ratio of hydroxyapatite and Fe_3O_4 of 2:1 in various contact time, pH, and initial concentration of phenol. Experiments were conducted with various contact time ranging from 15 to 120 minutes, using 50 mL of phenol having an initial concentration of 50 mg L^{-1} with an adsorbent weight of 0.1 g. The optimum pH of adsorption was determined by setting the experiments at pH varied from 2 to 10 using 0.1 M HCl and NaOH solution, whereas the optimization of initial concentration was studied through varying it from 10 to 90 mg L^{-1}. The adsorption capacity was calculated using the following equation:

$$q_e = \frac{C_o - C_e}{W} \text{ x } 100 \quad (1)$$

...where: C_o and C_e are the initial and final concentration of phenol after the equilibrium is achieved (mg L^{-1}), W is the weight of adsorbent (g).

Results and Discussion

Characterization of Hydroxyapatite-PEG/Fe_3O_4 Composites

FTIR spectra of hydroxyapatite and hydroxyapatite-PEG/Fe_3O_4 prepared at ratios of 3:1; 2:1 and 1:1 are shown in Fig. 1. The hydroxyl groups (OH-stretching vibration) appear around 3400 cm^{-1}, indicated by the sharp and broad peaks of the OH groups of PEG and hydroxyapatite. The broad peaks at 1620-1630 cm^{-1} belong to H_2O, while the Fe_3O_4 characteristic spectra are revealed at 560-590 cm^{-1}. The peaks at the same wavenumber region, belonging to hydroxyapatite around 569 and 601 cm^{-1}, represent phosphate vibrations (O–P–O). The phosphate groups (P–O) present at

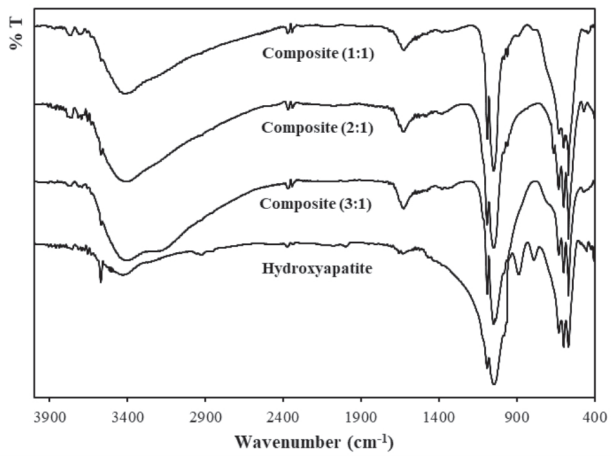

Fig. 1. FTIR spectra of hydroxyapatite and hydroxyapatite-PEG/Fe_3O_4 composites.

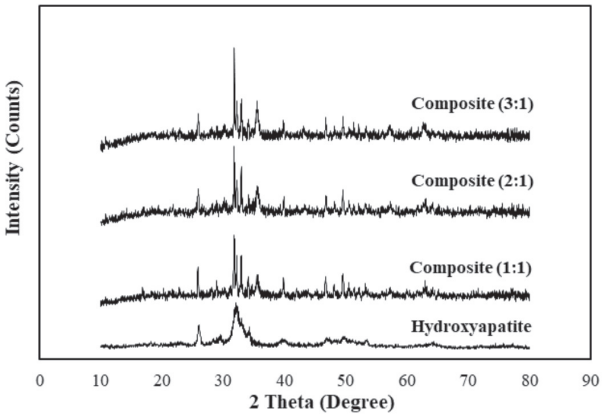

Fig. 2. XRD spectra of hydroxyapatite and hydroxyapatite-PEG/Fe_3O_4 composites.

1151-1121 cm^{-1} can also be identified as hydroxyapatite [8].

XRD patterns of hydroxyapatite and the composites are shown in Fig. 2. Hydroxyapatite has several characteristic peaks at 2θ as cited on JCPDS 09-423 (2θ = 31.7, 39.8, 46.7, 49.4, and 53.1°). After being made in composites, two more peaks appear at 2θ = 35.5 and 62.7°, which belong to Fe_3O_4. The intensity of these two peaks becomes intense as Fe_3O_4 increases. The XRD patterns of the composites can be assumed containing both hydroxyapatite and Fe_3O_4 patterns without any changing or shifting $2q$. The formation of hydroxyapatite-PEG/Fe_3O_4 composites is considered as a physical process.

The surface morphology of materials is presented by the SEM image with a 20,000× magnification in Fig. 3. Hydroxyapatite has a porous and heterogeneous surface, while the composites look having smoother surfaces, especially when Fe_3O_4 increases. The particles of Fe_3O_4 can enter hydroxyapatite pore and stick on its surface. On the composite having a ratio of 1:1, the SEM image shows fine particles distributed uniformly on the hydroxyapatite surface. The composition of hydroxyapatite and the composite elements analyzed using EDS, is shown in Table 1. Fe, in the composites, increases along with the increase of Fe_3O_4.

The composite having a ratio of hydroxyapatite to Fe_3O_4 of 1:1 provides the highest saturation magnetization, as shown in Fig. 4. Data in Table 2 reveal the values of surface area, pore-volume, and average pore diameter. The high saturation magnetization emanates from Fe_3O_4 contained in the composite. A large amount of Fe_3O_4 that is spread and entering and adhering to the pores and surface of hydroxyapatite causes the saturation magnetization to increase and, conversely, causes the surface area of hydroxyapatite to decrease. Hu et al. [21] reported that the saturation magnetization of Fe_3O_4 is 75.3 emu g^{-1}. In general, compositing, including coating, materials, tend to reduce the magnetic properties, as confirmed by We et al. [22]. The authors made Fe_3O_4 coated

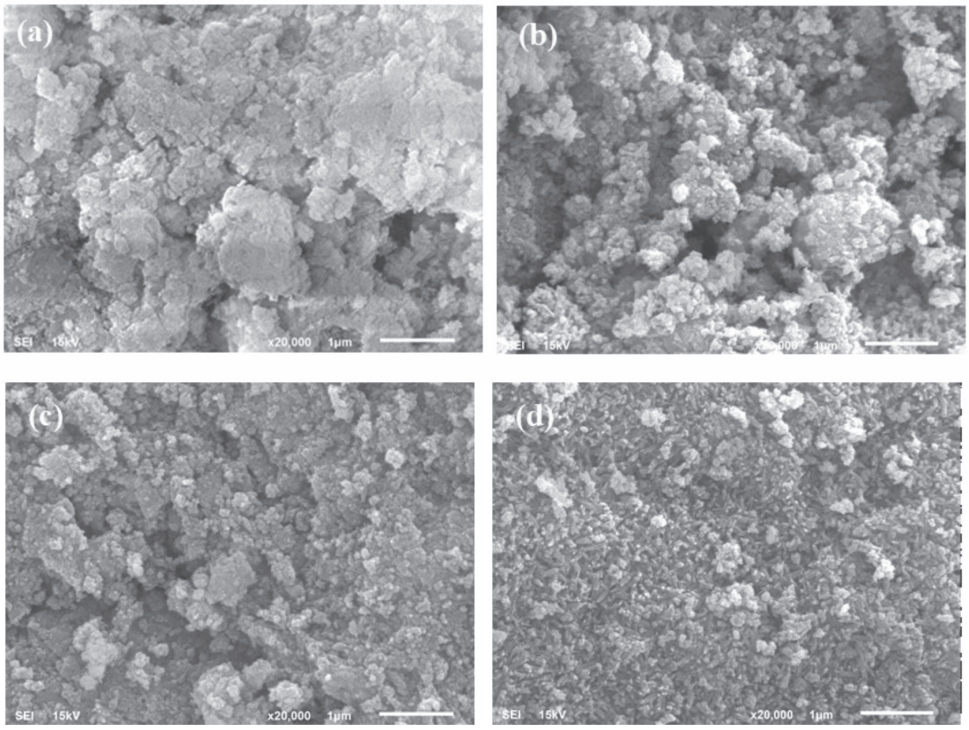

Fig. 3. Morphology of a) hydroxyapatite and of hydroxyapatite-PEG/Fe_3O_4 composites with ratios of b) 3:1, c) 2:1 and d) 1:1.

Table 1. Elemental composition of hydroxyapatite and hydroxyapatite-PEG/Fe_3O_4 composites analyzed by EDS.

Element	Mass (%)			
	Hydroxyapatite	Composite (3:1)	Composite (2:1)	Composite (1:1)
Ca	34.60	26.83	20.82	16.62
P	15.85	12.47	9.48	7.90
O	49.55	41.18	38.18	36.86
Fe	-	12.67	21.96	26.76
C	-	6.85	9.56	11.86

with sodium citrate and oleic acid and finally found out the decrease of the saturation magnetization. The surface areas of the composites with ratios of 3:1 and 2:1 showed an insignificant difference, namely 245.2 and 237.3 $m^2 g^{-1}$, while the other one with a ratio of 2:1 showed a higher saturation magnetization of 57.8 emu g^{-1}, thus used in the adsorption experiment.

Effects of Contact Time, Solution pH, and Initial Concentration

The effects of contact time, solution pH, and initial concentration on the adsorption capacity of hydroxyapatite and hydroxyapatite-PEG/Fe_3O_4

Table 2. The values of BET surface area, pore-volume, and average pore diameter of hydroxyapatite and hydroxyapatite-PEG/Fe_3O_4 composites.

Adsorbent	BET surface area ($m^2 g^{-1}$)	Pore volume ($cm^3 g^{-1}$)	Average pore diameter (nm)
Hydroxyapatite	264.6	0.214	4.45
Composite (3:1)	245.2	0.183	5.62
Composite (2:1)	237.3	0.172	5.82
Composite (1:1)	201.3	0.142	6.21

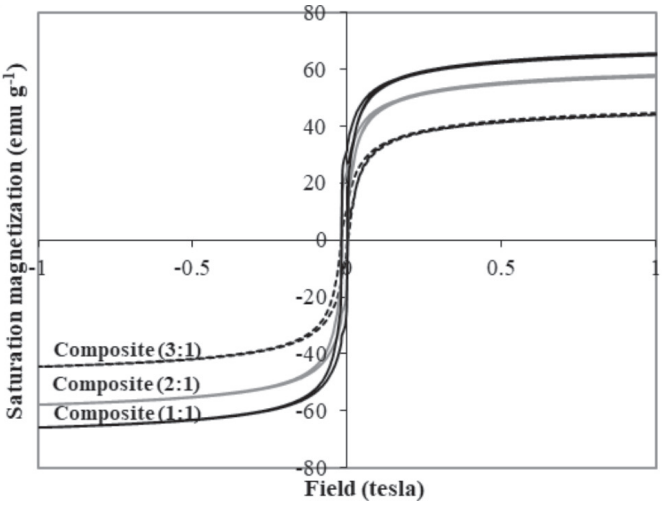

Fig. 4. VSM curves of hydroxyapatite-PEG/Fe_3O_4 composites.

composite are depicted in Fig. 5. The adsorption capacities of both adsorbents show a tendency to increase following the contact time. The longer the interaction of the adsorption process, the more active the sites on the adsorbent to interact with phenol. The composite achieved adsorption equilibrium after 45 minutes, while hydroxyapatite did after 75 minutes (Fig. 5a). Once the equilibrium was reached, contact time did not affect further on adsorption capacity. In this case, our study achieved equilibrium faster than others using the same adsorbates as phenol. Acuntion et al. [4], using carbon nanomaterial, and Polat et al. [21], using lignite, reported that adsorption equilibrium is achieved in longer contact time.

Solution pH plays an essential role in phenol adsorption [23]. pH ranging from 2 to 10 was used in this report, as displayed in Fig. 5b). Adsorption capacity at a pH range of 2-6 provided higher values compared to a pH range of 7-10. At a pH range of 2-5, the adsorption capacity was relatively constant. Protonation of hydroxyapatite occurred at low pH created a positive charge on its surface, leading hydroxyapatite and phenol to interact with each other through attraction force [24]. Three variables affecting the adsorption of phenol at varying levels of pH were (i) phenol and hydroxyapatite, becoming negatively charged at basic condition, thus not supporting the adsorption process, (ii) adsorption mechanism occurring through H-bond formation between H-atom on phenol and O-atom on hydroxyapatite or between H-atom on hydroxyapatite and O-atom on phenol. Phenol is known as weak acid having pKa of 9.89, in which at pH>pKa, H-bond is unlikely to form and (iii) folic acid has a lower solubility in acidic condition [4, 23, 25]. Fig. 6. illustrates the interaction between hydroxyapatite-PEG/Fe_3O_4 composites and phenols.

The effect of the initial concentration of phenol explains its mass transfer between its liquid and solid phases. Phenol initial concentration, in this study, ranged from 10 to 90 mg L^{-1} with a volume of 50 mL,

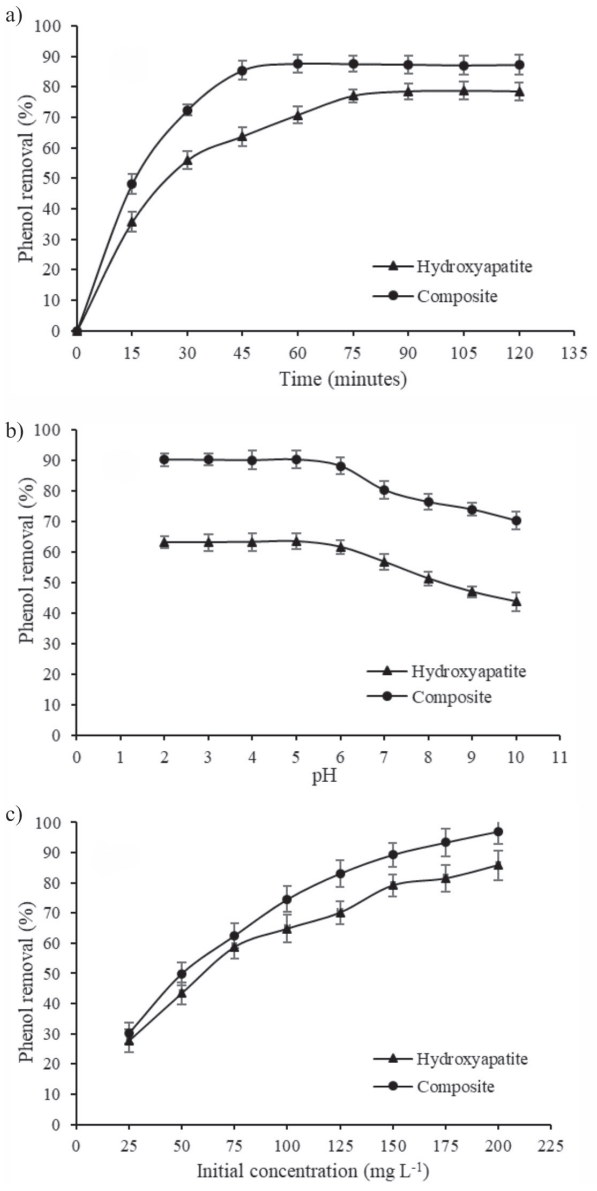

Fig. 5. Effects of a) contact time, b) solution pH, and c) initial concentration.

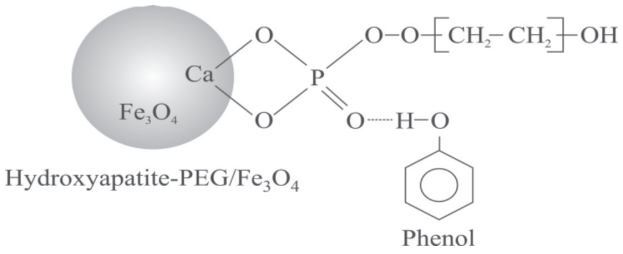

Fig. 6. Interaction of hydroxyapatite-PEG/Fe_3O_4 composites with phenols.

the weight of adsorbent of 0.1 g, and pH of 5 at room temperature. Fig. 5c) shows that initial concentration and adsorption capacity are correlated proportionally. Other studies using *Luffa cylindrica* [1], lignite [26], and activated carbon reported having similar results [27]. In this study, both hydroxyapatite and composites have a similar tendency.

Adsorption Kinetics

Rate constant and reaction order are important variables on describing adsorption mechanisms and chemical reactions. This experiment used the pseudo-first order and pseudo-second order models. The former is expressed in the following equation [28]:

$$\frac{1}{q_t} = \frac{k_1}{q_1}\frac{1}{t} + \frac{1}{q_1} \quad (2)$$

...where q_t and q_1 are the amounts of phenol adsorbed at t time and at equilibrium condition (mg g^{-1}), respectively, while k_1 is the pseudo-first order constant (min^{-1}) calculated via slope and intercept of a graph plotted between $1/q_t$ vs $1/t$.

The pseudo-second order model is expressed by the following equation:

$$\frac{t}{q_t} = \frac{1}{k_2 {q_2}^2} + \frac{t}{q_2} \quad (3)$$

...where q_2 is the amount of phenol adsorbed at equilibrium (mg g^{-1}), k_2 is the pseudo-second order constant (g mg^{-1} min^{-1}) obtained from the slope and intercept plot of t/q_t vs t.

Fig. 7 displays adsorption kinetics of phenol using hydroxyapatite and the composite. Table 3 presents the calculation results of kinetics parameters. The value of R^2 on the pseudo-second order model is higher than that on the other one for both hydroxyapatite and the composite. The pseudo-second order model, hence, best describes the adsorption mechanism of phenol on hydroxyapatite and the composite. The values of k_2 on phenol adsorption by using hydroxyapatite and the composite are $10.8.10^{-5}$ and $8.2.10^{-5}$ (g mg^{-1} min^{-1}), indicating that the adsorption began at a fast rate.

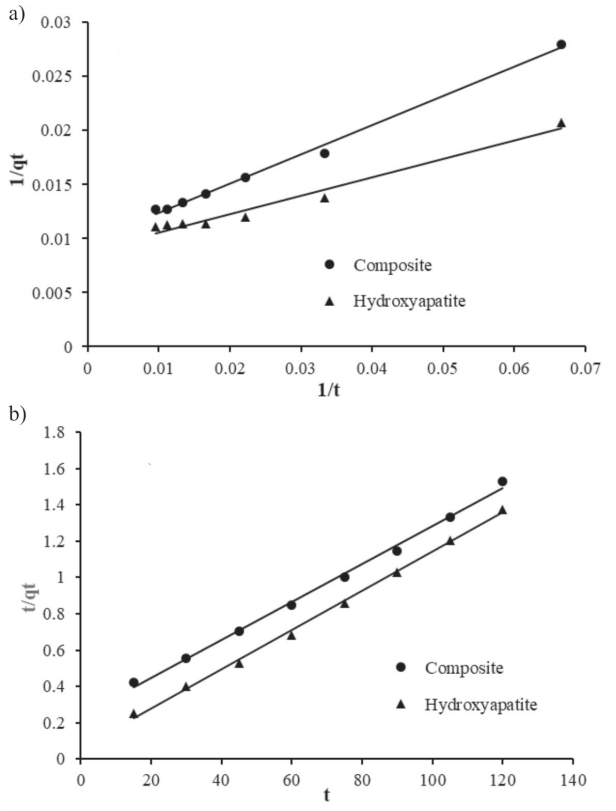

Fig. 7. Plot results from the calculation of the a) pseudo-first order and b) pseudo-second order of phenol adsorption onto hydroxyapatite and hydroxyapatite-PEG/Fe_3O_4 composite.

Adsorption Isotherm

This study used phenol concentration varied to obtain adsorption isotherm, employing two types of isotherm, namely the Langmuir and Freundlich isotherms, the former of which assumes that adsorption occurs homogeneously on all active sites of the adsorbents. The linear correlation of the Langmuir isotherm is expressed by the following equation [2]:

$$\frac{1}{q_e} = \frac{1}{K_L q_m}\frac{1}{C_e} + \frac{1}{q_m} \quad (4)$$

...where q_e and q_m are the amounts of phenol adsorbed at equilibrium and at maximum condition capacity (mg g^{-1}), respectively, while C_e is phenol concentration within solution at equilibrium (mg L^{-1}), and K_L is the Langmuir constant (L g^{-1}). The Feasibility of the Langmuir isotherm is expressed in dimensionless constant separations, written as the following equation:

$$R_L = \frac{1}{1+K_L C_o} \quad (5)$$

If R_L is more than 1 (R_L>1), then the Langmuir isotherm is unfavourable. If it is linear (R_L = 1) then Langmuir isotherm is favourable (0<R_L<1). Whereas, R_L = 0 indicates an irreversible process.

Table 3. Kinetics parameters of phenol adsorption on hydroxyapatite and hydroxyapatite-PEG/Fe_3O_4 composite.

Adsorbent	Pseudo-first order			Pseudo-second order		
	k_1 (min^{-1})	q_1 (mg g^{-1})	R^2	k_2 (g mg^{-1} min^{-1})	q_2 (mg g^{-1})	R^2
Hydroxyapatite	23.39	103.69	0.964	$10.8.\ 10^{-5}$	96.13	0.996
Composite (2:1)	19.15	112.35	0.975	$8.2.10^{-5}$	110.13	0.998

The Freundlich isotherm assumes that adsorbents have heterogeneous surfaces and that active site is not energetically equivalent. The linearity of this approach is expressed by:

$$ln\ q_e = ln\ K_f + \frac{1}{n}\ln C_e \quad (6)$$

K_f is the Freundlich isotherm constant (L/mg) and n represents empirical parameters correlated to adsorption intensity. The value of $\frac{1}{n}$ at a range of $0.1<\frac{1}{n}<1$ provides an indication that adsorption process is favourable [29].

Table 4 shows parameters for the Langmuir and Freundlich isotherms on phenol adsorption using hydroxyapatite and hydroxyapatite-PEG/Fe_3O_4 composite. Coefficient correlation value (R^2) on both isotherms are above 0.9. However, the Langmuir isotherm shows R^2 higher than that of the Freundlich isotherm. This finding indicates that adsorption of phenol on hydroxyapatite and the composite the best fit with Langmuir isotherm. The maximum adsorption capacity of the hydroxyapatite is 88.49 mg g^{-1}, smaller than that of hydroxyapatite-PEG/Fe_3O_4 composite, which is 95.24 mg g^{-1}, indicating that the presence of Fe_3O_4 lowers the adsorption capacity due to the lower surface area available. These results furthermore confirmed that this difference of adsorption capacities of the composite is relatively higher than that of uncomposite materials reported by Jiang et al. [30], in which the adsorption capacity of activated carbon/$NiFe_2O_4$ is 182.82 mg g^{-1} and that of activated carbon is 136.61 mg g^{-1} while used for the adsorption of methyl orange dye. A magnetic adsorbent also more efficient because it can be separated simply by using a permanent magnet and no filtration process is needed. The R_L values at an initial concentration of 10 mg L^{-1} were 0.524 for hydroxyapatite and 0.103 for composite (R_L<1), both of which indicated a favorable adsorption process.

Table 5 presents the comparison of the adsorption capacities of several adsorbents in phenol removal. According to the table, the adsorption capacities obtained in this research are relatively higher than those of some adsorbents reported. The adsorption capacity of hydroxyapatite-PEG/Fe_3O_4 composite indeed higher than that of hydroxyapatite and the composite has a benefit in the form of efficient separation from the solution and ease to regain using a permanent magnet.

Thermodynamics Adsorption

To determine the effect of temperature on the adsorption of phenol using hydroxyapatite and hydroxyapatite-PEG/Fe_3O_4 composite, changes in free energy (ΔG^0), enthalpy (ΔH^0), and entropy (ΔS^0) are calculated. The change in free energy can be calculated from the equation:

$$\Delta G^0 = -RTlnK_0 \quad (7)$$

...where R is the gas constant (8.314 JK mol^{-1}), T is the temperature (K), and K_0 is the equilibrium constant. Entalpy and entrophy are determined using the equation:

$$lnK_0 = \frac{\Delta S^0}{R} - \frac{\Delta H^0}{RT} \quad (8)$$

The value of ΔH^0 dan ΔS^0 can be calculated from the slope and intercept based on plot lnK_0 versus 1/T. The calculation result of ΔG^0, ΔH^0 dan ΔS^0 are shown in Table 6.

The value of ΔG^0 in phenol adsorption using hydroxyapatite and hydroxyapatite-PEG/Fe_3O_4 composite has a negative value indicating that the adsorption process of phenol is feasible and spontaneous. The value of ΔG^0 increases with increasing

Table 4. Adsorption isotherm parameters of phenol adsorption on hydroxyapatite and hydroxyapatite-PEG/Fe_3O_4 composite.

Adsorbent	Langmuir			Freundlich		
	q_m (mg g^{-1})	K_L (L g^{-1})	R^2	K_f (mg g^{-1})	1/n (L g^{-1})	R^2
Hydroxyapatite	88.49	0.031	0.996	8.17	0.487	0.971
Composite (2:1)	95.24	0.018	0.997	5.79	0.516	0.981

Table 5. Adsorption capacities of several adsorbents in phenol adsorption.

Adsorbent	Adsorption capacity (mg g^{-1})	Reference
Luca cylindrica fibers	9.25	[1]
Carbon naomaterials	25.125	[4]
Hydroxyapatite	10.33	[2]
Bentonite	0.247	[31]
Kaolinite Chitin Chitosan	0.468 1.96 1.26	[31] [32] [32]
Natural clay	15	[33]
Hexadecyltrimethylammonium–bentonite	18.8	[34]
Hydroxiapatite	88.49	In this study
Hydroxypatite-PEG/Fe_3O_4 composite (2:1)	95.24	In this study

Table 6. Thermodynamic parameters of phenol adsorption on hydroxyapatite and hydroxyapatite-PEG/Fe_3O_4 composite.

	Temperature (K)	ΔG^0 (kJ mol^{-1})	ΔH^0 (kJ mol^{-1})	ΔS^0 (J mol^{-1} K^{-1})
Hydroxya-patite	298	-9.498	-4.373	17.197
	303	-9.584		
	308	-9.670		
Composite (2:1)	298	-9.026	-4.136	16.411
	303	-9.108		
	308	-9.191		

temperature, represents the strength of attraction so that the adsorption capacity increases. In general, the value of ΔG^0 ranges at -20-0 kJ mol^{-1} for physical adsorption [35]. A negative ΔH^0 value indicates that the adsorption process is exothermic, whereas a positive ΔS^0 indicates the irregularity of phenol adsorption on the adsorbent surface.

Conclusions

Hydroxyapatite-PEG/Fe_3O_4 composites were successfully prepared via co-precipitation method. The surface area of the composite was lower than that of hydroxyapatite, but the magnetic properties became higher as Fe_3O_4 increased. The adsorbent composite made at a ratio of hydroxyapatite and Fe_3O_4 of 2:1 was chosen for this study of phenol adsorption because it has both high surface area and magnetic properties. The adsorption capacities of both untreated hydroxyapatite and hydroxyapatite-PEG/Fe_3O_4 composite are 88.49 and 95.24 mg g^{-1}. Thermodynamic calculations show that the adsorption of phenols using hydroxyapatite and hydroxyapatite-PEG/Fe_3O_4 is spontaneous and exothermic. The hydroxyapatite-PEG/Fe_3O_4 composite can be an alternative of potential adsorbent due to its fast adsorption process and ease of separation using a permanent magnet without filtration, thus lowering the separation costs.

Acknowledgments

The authors would like to thank the Indonesian Ministry of Research, Technology, and Higher Education of Republic Indonesia that provided funding through PDUPT grant on year 2019 No. 0060.09/UN9/SB3/LP2M/PT/2019. We also thank Rima Melati for the characterization of material by XRD, FTIR and SEM-EDS

Conflict of Interest

The authors declare no conflict of interest.

References

1. ABDELWAHAB O., AMIN N.K. Adsorption of phenol from aqueous solutions by Luffa cylindrica fibers: Kinetics, isotherm and thermodynamic studies. Egyptian Journal of Aquatic Research, **39** (4), 215, **2013**.
2. LIN K., PAN J., CHEN Y., CHENG R., XU X. Study the adsorption of phenol from aqueous solution on hydroxyapatite nanopowders. Journal of Hazardous Materials, **161** (1), 231, **2008**.
3. TURCO A., MONTEDURO, A.G., MAZZOTTA E., MARUCCIO G., MALITESTA C. An innovative porous nanocomposite material for the removal of phenolic compounds from aqueous solutions. Nanomaterials, **8** (34), 1, **2018**.
4. ASUNCION M.L., MENDIETA V.S., HERNANDEZ, A.L.M., CASTANO V.M., SANTOS, C.V. Adsorption of phenol from aqueous solutions by carbon nanomaterials of one and two dimensions: kinetic and equilibrium studies. Journal of Nanomaterials, **2015**, 1, **2015**.

5. ZHOU L., CAO H., DECORME C., XIE Y., Phenolic compounds removal by wet oxidation based processes. Frontiers of Environmental Science and Engineering, **12** (1), 1, **2018**.
6. MAKOOTIAN M., HEIDARI M.R. Removal of phenol from steel wastewater by combined electrocoagulation with photo-Fenton. Water Science and Technology, **78** (6), 1260, **2018**.
7. HUSSAIN A., DUBEY S.K., KUMAR V. Kinetic study for aerobic treatment of phenolic wastewater. Water Resources and Industry, **11** (5), 81, **2015**.
8. LI J., ZHAO H., MA C., HAN Q., LI M., LIU H. Preparation of Fe_3O_4@polyoxometalates nanocomposites and their efficient adsorption of cationic dyes from aqueous solution. Nanomaterials, **9** (4), 1, **2019**.
9. ZHUANG F., TAN R., SHEN W., ZHANG X., XU W., SONG W. Monodisperse magnetic hydroxyapatite/Fe_3O_4 microsphere for removal of lead (II) from aqueous solution. Journal of Alloys and Compounds, **637**, 531, **2015**.
10. FATIMAH I., AULIA G.R., PUSPITASARI, W., NURILLAHI R., SOPIA L., HERIANTO R. Microvawe synthesis hydroxyapatite from paddy field snail (Pila ampullaceal) shell for adsorption of bichromate ion. Sustainable Environment Research, **28**, 462, **2018**.
11. ICONARU S.L., HEINO M.M., GUEGEN R., PREDOI V., PRODAN A.M., PREDOI D. Removal of zinc ions hydroxyapatite and study of ultrasound behavior of aqueous media. MaterIALS, **11** (8): 1, **2018**.
12. HARIANI P.L., MURYATI., SAID M. Kinetic and thermodynamic adsorption of nickel (II) onto hydroxyapatite prepared from snakehead (Channa striata) fish bone. Mediterranean Journal of Chemistry, **9** (2), 85, **2019**.
13. ZHANG M., MAO Y., WANG W., YANG S., SONG Z., ZHAO X. Coal fly ash/$CoFe_2O_4$ composites: a magnetic adsorbent for the removal of malachite green from aqueous solution. RSC Advances, **6**, 93564, **2016**.
14. ZHANG G., QU J., LIU H., COOPER A.T., WU R. $CuFe_2O_4$/activated carbon composite: A novel magnetic adsorbent for the removal of acid orange II and catalytic regeneration. Chemosphere, **68** (6), 1058, **2007**.
15. HARIANI P.L., FAIZAL M., RIDWAN, MARSI, SETIABUDIDAYA D. Removal of Procion Red MX-5B from songket's industrial wastewater in South Sumatra Indonesia using activated carbon-Fe_3O_4 composite. Sustainable Environment Research, **28**, 158, **2018**.
16. FU H., DING X., REN C., Li W., WU H., YANG H. Preparation of magnetic porous $NiFe_2O_4/SiO_2$ composite xerogels for potential application in adsorption of Ce(IV) ions from aqueous solution. RSC Advances. **7**, 16513, **2017**.
17. FRONCZAK M., STRACHOWASKI P., KASZUWARA W., BYZTRZEJEWKI M. Magnetic composite adsorbents of phenolic compounds with superior corrosion resistance. Separation Science and Technology, **54** (14), 2252, **2019**.
18. KONATE A., HE X., ZHANG Z., MA Y., ZHANG P., ALUNGONGO GM., RUI T. Magnetic (Fe_3O_4) nanoparticles reduce heavy metals uptake and mitigate their toxicity in wheat seedling. Sustainability, **9** (790), 1, **2017**.
19. KOESNARPADI S, SANTOSA S.J., SISWANTA D., RUSDIARSO B. Humic acid coated Fe_3O_4 nanoparticle for phenol sorption. Indonesian Journal of Chemistry, **17** (2), 274, **2017**.
20. ABBOUD M., YUSSEF S., PODLECKI J., HABCHI R., GERMANOS G., FOUCARAN A. Superparamagnetic Fe_3O_4 nanoparticles, synthesis and surface modification. Materials Science Semiconductor Processing, **39**, 641, **2015**.
21. HU P., KANG L., CHANG T., YANG F., WANG H., ZHANG Y., YANG J., WANG K., DU J., YANG Z. High saturation magnetization Fe_3O_4 nanoparticles by one step reduction method in autoclave. Journal of Alloys and Compounds, **728**, 88, **2017**.
22. WEI Y., HAN B., HU X., LIN Y., WANG X., DENG X. Synthesis of Fe_3O_4 nanoparticles and their magnetic properties. Procedia Engineering, 27, 632, **2012**.
23. GE M., WANG X., DU M., LIANG G., HU G., ALAM J.S.M. Adsorption analyses of phenol from aqueous solutions using magadiite modified with organo-functional groups: kinetic and equilibrium studies. Materials, **12** (1), 96, **2019**.
24. XIAOLI C., YOUCAI Z. Adsorption of phenolic compound by aged-refuse. Journal of Hazardous Materials, **137** (1), 410, **2006**.
25. WANG X. Preparation of magnetic hydroxyapatite and their use as recyclable adsorbent for phenol in wastewater. Clean-Soil Air Water, **39** (1), 13, **2011**.
26. POLAT H., MOLVA M., POLAT M. Capacity and mechanism of phenol adsorption on lignite. International Journal of Mineral Processing, **79** (4), 264, **2006**.
27. GUNDOGDU A., DURAN C., SENTURK H.B, SOYLAK M., Ozdes D, SERENCAM H., IMAMOGLU M. Adsorption of phenol from aqueous solution on a low cost activated carbon produced from tea industry waste: equilibrium, kinetic, and thermodynamic study. Journal of Chemical and Engineering Data, **57** (10), 2733, **2012**.
28. KALAIVANI S.S., VIDHYADEVI T., MURUGESAN A., BASKARALINGAM P., ANURADHA C.D., RAVIKUMAR l., SIVANESAN S. Equilibrium and kinetic studies on the adsorption of Ni(II) ion from an aqueous solution using activated carbon prepared from Theobroma caco (cocoa) shell. Desalination and water Treatment, **54** (6), 1629, **2015**.
29. DONG L., ZHU Z., QIU Y., ZHAO J. Removal of lead from aqueous solution by hydroxyapatite/magnetite composite adsorbent. Chemical Engineering Journal, **165** (3), 827, **2010**.
30. JIANG T., LIANG YD., HE Y., WANG Q. Activated carbon/NiFe2O4 magnetic composite: A magnetic adsorbent for the adsorption of methyl orange, Journal of Environmental Chemical Engineering, **3** (3), 1740, **2015**.
31. ALKARAM U.F., MUKHLIS A.A., Al-DUJAILI A.H. The removal of phenol from aqueous solution by adsorption using surfactant-modified bentonite and kaolinite. Journal of Hazardous Materials, **169 (1-3)**, 324, **2009**.
32. MILHOME M.A.L., KEUKELEIRE D., RIBERIO J.P., NASCIMENTO Rr.f., CARVALHO T.V., QUEIROZ D.C. Removal of phenol and conventional pollutants from aqueous effluent by chitosan and chitin. Quimica Nova, **32** (8), 2122, **2009**.
33. DJEBBAR M, DJAFRI F., BOUCHEKARA M. Adsorption of phenol on natural clay. 2012. Applied Water Science, **2**, 77–86, **2012**.
34. PLASKA A.G. Application of modified clay for removal of phenol and PO_4^{3-} ions from aqueous solutions. Adsorption Science and Technology, **35** (7-8), 692, **2017**.
35. HUANG C.H., CHANG K.P., OU H., CHIANG Y.C., WANG C.F. Adsorptions of cationic dyes onto mesoporous silica. Microporous and Mesoporous Materials. **141** (1-3), 102, **2011**.